DOI: 10.1002/ejic.200900013

Synthesis, Structure, Conductivity, and Calculated Nonlinear Optical Properties of Two Novel Bis(triphenylphosphane)copper(I) Dithiocarbamates

Abhinav Kumar,[a] Heike Mayer-Figge,[b] William S. Sheldrick,[b] and Nanhai Singh*[a]

Dedicated to the late A. Marshall

Keywords: Copper / Dithiocarbamate / Density functional calculations / Semiconductivity / Nonlinear optics

A centrosymmetric binuclear [{Cu(PPh$_3$)$_2$}$_2$(piperzdtc)] (**1**) [piperzdtc^{2-} = piperazinebis(dithiocarbamate)] and another mononuclear [{Cu(PPh$_3$)$_2$}(BzMedtc)] (**2**) (BzMedtc$^-$ = *N*-benzyl-*N*-methyldithiocarbamate) complex have been synthesized and characterized by elemental analyses, IR, ^{1}H, ^{13}C, and ^{31}P NMR spectroscopy and by X-ray crystallography. The nonlinear optical properties of **2** have been investigated by density functional theory and its electronic absorption bands have been assigned by time-dependent density functional theory (TD-DFT). Both complexes are weakly conducting ($\sigma_{rt} \approx 10^{-8}$ S cm^{-1}) because of the absence of M···S/S···S intermolecular stacking and exhibit semiconductivity with band gaps of 0.94 and 1.24 eV, respectively.

Introduction

The chemistry of transition-metal 1,1- and 1,2-dithio complexes in general is increasingly attracting intensive attention due to recognition of their useful physico-chemical properties such as solid-state conductivity, nonlinear optical (NLO) and photoluminescent, molecular magnetism, and multifarious chemistry.[1]

The renaissance of the dithiocarbamate ligand resulted in a large number of mono- and bimetallic coordination compounds that exhibited interesting structural motifs and properties.[1–3] The avid interest in the dithiocarbamate complexes stems from their ability to stabilize unusual high oxidation states of transition metals [e.g. iron(IV), copper(III), nickel(IV), and gold(III)] and their interesting electrochemical as well as optical properties and numerous industrial applications such as lubricants, antioxidants, fungicides, accelerators for rubber vulcanization, and as photoluminescent materials.[4,5] These are as a result of the delocalization that the ligand dithiocarbamate provides in contrast to other uninegative 1,1-dithio ligands (e.g. xanthates and dithiophosphates) and consequently high electron density that the sulfur donors present.[6]

Interestingly, despite synthetic versatility and practical applications only a few preliminary reports have appeared on the bidentate *N*-benzyl-*N*-methyldithiocarbamate[7] and polydentate ligand piperazinebis(dithiocarbamate)[8] complexes, the latter becoming one of the scaffolds of choice for construction of the bimetallic ligand system. Also, because of the usefulness of bulky tertiary phosphane ligands when coordinated to transition-metal ions for potential catalytic reactions[9] owing to their larger steric demand and σ-donor and π-acceptor ability, triphenylphosphane (PPh$_3$) has been used in the preparation of these complexes. With these aspects in mind and in the quest for interesting molecular conducting and nonlinear optical properties we herein report the synthesis, characterization, conducting, and optoelectronic properties of a mononuclear and another binuclear complex resulting from the reaction of bis(triphenylphosphane)copper(I) with dithiocarbamate ligands (Figure 1). Density functional theory calculations have been performed in order to interpret the nonlinear optical properties of the complexes. The electronic absorption bands have been assigned by employing time-dependent density functional theory (TD-DFT).

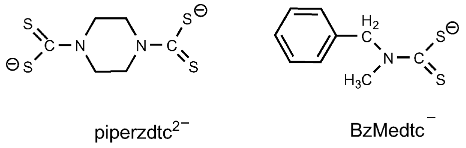

piperzdtc^{2-} BzMedtc$^-$

Figure 1. Structure of the ligands.

---

[a] Department of Chemistry, Faculty of Science, Banaras Hindu University,
Varanasi 221005, India
Fax: +91-542-2386127
E-mail: nsingh@bhu.ac.in
[b] Lehrstuhl für Analytische Chemie, Ruhr-Universität Bochum,
44780 Bochum, Germany

Supporting information for this article is available on the WWW under http://dx.doi.org/10.1002/ejic.200900013.

Results and Discussion

The complexes [{Cu(PPh$_3$)$_2$}$_2$(piperzdtc)] (**1**) and [{Cu(PPh$_3$)$_2$}(BzMedtc)] (**2**) were synthesized by gradual addition under stirring of a methanol solution of the ligand salts Na$_2$piperzdtc or NaBzMedtc to the dichloromethane solution of [Cu(PPh$_3$)$_2$(NO$_3$)] in appropriate molar ratios at 0 °C.

$$\textbf{1.}\ 2[\mathrm{Cu(PPh_3)_2}]\mathrm{NO_3} + \mathrm{Na_2piperzdtc} \xrightarrow[\mathrm{CH_2Cl_2}]{\mathrm{CH_3OH,}} [\{\mathrm{Cu(PPh_3)_2}\}_2(\mathrm{piperzdtc})] + 2\mathrm{NaNO_3}$$

$$\textbf{2.}\ [\mathrm{Cu(PPh_3)_2}]\mathrm{NO_3} + \mathrm{NaBzMedtc} \xrightarrow[\mathrm{CH_2Cl_2}]{\mathrm{CH_3OH,}} [\{\mathrm{Cu(PPh_3)_2}\}(\mathrm{BzMedtc})] + \mathrm{NaNO_3}$$

Spectroscopy

The IR spectra of both **1** and **2** show a distinct vibrational band at 1091 cm^{-1} that is associated with the symmetric bidentate ν(CS$_2$) vibration of the dithiocarbamate ligands. The band near 1384 cm^{-1} for both **1** and **2** is characteristic of the thioureide vibration and is associated with ν(C–N) which is appreciably higher than for the free ligand thereby indicating a significant increase in the partial double-bond character in the C–N bond.

The purity and composition of both the compounds have been checked by NMR spectroscopy. Both the compounds display sharp ^{1}H NMR signals that integrate well with the corresponding hydrogen atoms. A significant shift of δ = 10 ppm in the ^{13}C NMR resonances for the CS$_2$ carbon in both complexes as compared to the free ligand indicates M–S bonding. The signals in the δ = 127–136 ppm range correspond to the aromatic protons of the triphenylphosphane ligand for both **1** and **2** and the benzyl group for **2**. Only one singlet was observed in the ^{31}P NMR spectra of **1** (δ = –1.76 ppm) and **2** (δ = 0.19 ppm) revealing that the phosphorus donors are only bonded to the Cu atom. Appearance of sharp peaks in the ^{1}H and ^{13}C NMR spectra confirms the presence of diamagnetic Cu$^{\mathrm{I}}$ in both **1** and **2**.

Single-Crystal Structure

The single crystals of both **1** and **2** were obtained by slow evaporation of the reaction mixture. The immediate coordination geometries about the Cu atoms in the binuclear **1** (Figure 2) and mononuclear **2** (Figure 3) are defined by the two phosphorus atoms of the monodentate triphenylphosphane and the atoms S(1) and S(2) of the bidentate dithiocarbamate ligands in which the Cu atom is located at the center of a distorted tetrahedral environment (see Figures 2 and 3). The Cu(1)–S(1) and Cu(1)–S(2) bond lengths for **1** are 2.402(6) and 2.401(6) Å, respectively, while for **2** these are 2.402(14) and 2.398(12) Å, respectively, thereby reflecting the symmetrical bidentate coordination of the dithio ligand with the Cu atoms. In the case of **1** the bond angles P(1)–Cu(1)–S(1), P(1)–Cu(1)–S(2), P(2)–Cu(1)–S(1), and P(2)–Cu(1)–S(2) are 111.82(2)°, 116.57(2)°, 120.94(2)°, and 106.43(2)°, respectively, while for **2** these are 109.71(5)°, 110.12(5)°, 106.64(5)°, and 118.32(5)°, respectively. The bite angles S(1)–Cu(1)–S(2) are 75.41(2)° and 75.29(4)° for **1** and **2**, respectively. The deviation from planarity of atoms Cu(1), S(1), S(2), and C(1), defining the chelate ring are 0.03, 0.05, 0.05, and 0.07 Å, respectively for **1**, whereas for **2**, these are 0.02, 0.03, 0.03, and 0.04 Å, respectively. For **1** the angle between the least square plane, i.e. Cu(1), S(1), S(2), and C(1) and that through the plane formed by P(1), Cu(1), and P(2) is 81.92° and in the case of **2** this angle is 85.28°, both of which indicate that the two planes are approximately perpendicular to each other. In the case of **1** the angle between the plane formed by the carbon atoms of the piperazine ^{4}C chair and the chelate ring formed by the Cu(1), S(1), S(2), and C(1) atoms is 68.53°. Additionally for the binuclear complex **1** the distance between the two parallel planes formed by Cu(1), S(1), S(2), and C(1) at the opposite ends is 2.36 Å. The C(1)–N bond lengths in **1** and **2** are 1.342(3) and 1.336(5) Å, respectively. This is indicative of partial double bond character as these values are intermediate between those of the C–N (1.47 Å) and C=N (1.28 Å) bonds. Selected bond lengths and bond angles are given in Table 1.

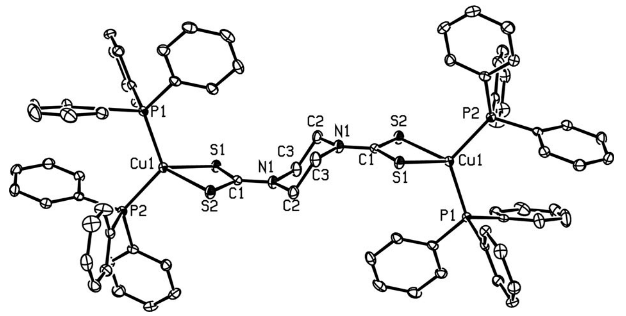

Figure 2. ORTEP diagram for **1** at 50% probability level. Hydrogen atoms are removed for clarity.

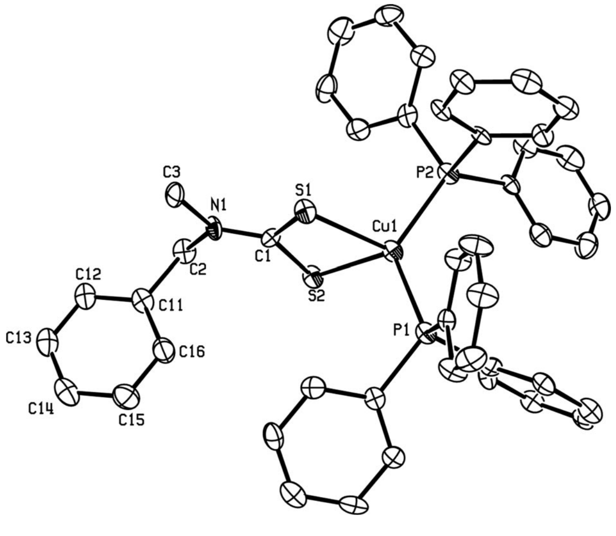

Figure 3. ORTEP diagram for **2** at 50% probability level. Hydrogen atoms and solvent molecule are removed for clarity.

Table 1. Selected bond lengths [Å] and angles [°] for the complexes.

Bond length [Å]	1	2
Cu(1)–P(1)	2.256(6)	2.2378(14)
Cu(1)–P(2)	2.244(6)	2.2603(13)
Cu(1)–S(1)	2.402(6)	2.402(14)
Cu(1)–S(2)	2.401(6)	2.398(12)
S(1)–C(1)	1.721(2)	1.708(4)
S(2)–C(1)	1.715(2)	1.729(5)
N(1)–C(1)	1.342(3)	1.336(5)
Bond angle [°]		
P(2)–Cu(1)–P(1)	118.06(2)	124.88(5)
P(2)–Cu(1)–S(2)	106.43(2)	118.32(5)
P(1)–Cu(1)–S(2)	116.57(2)	110.12(5)
P(2)–Cu(1)–S(1)	120.94(2)	106.64(5)
P(1)–Cu(1)–S(1)	111.82(2)	109.71(5)
S(1)–Cu(1)–S(2)	75.41(2)	75.29(4)
C(1)–S(1)–Cu(1)	83.09(8)	83.80(16)
C(1)–S(2)–Cu(1)	83.24(8)	83.51(14)
S(2)–C(1)–S(1)	117.52(13)	117.1(3)

Electronic Absorption Spectrum

The observed electronic absorption spectrum of **2** has been interpreted with the help of TD-DFT calculations. The electronic absorption spectrum of this complex (Figure 4) displays bands at 318, 264, and 231 nm which are assigned to the ligand-to-ligand charge transfer transition (LLCT) from the thioureide group of the dithiocarbamate ligand to the aromatic rings of triphenylphosphane and benzyl groups (Figure 5). The other transitions are also of ligand-to-ligand charge-transfer type. Calculated excitation energies, wavelength, oscillator strength, and major contribution are given in Table 2.

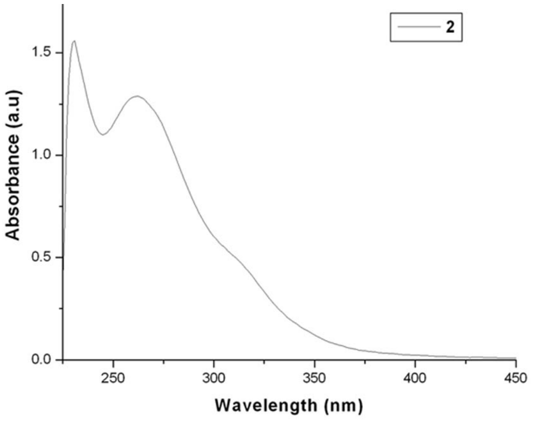

Figure 4. Electronic absorption spectrum for **2**.

Table 2. Selected excitation energies [eV], wavelength [nm], oscillator strengths (*f*), and transition type for **2**.

Excitation energy [eV]	Wavelength [nm]	Oscillator strength (*f*)	Major contribution
4.9762	249	0.0015	n→π* (PPh_3)
4.9489	252	0.0191	n→ π* (Benzyl)
4.6036	269	0.0148	n→π* (PPh_3)
4.2352	293	0.0546	n→π* (PPh_3)
3.9796	304	0.0397	imide→π* (PPh_3)
3.8984	318	0.0379	n→π* (PPh_3)

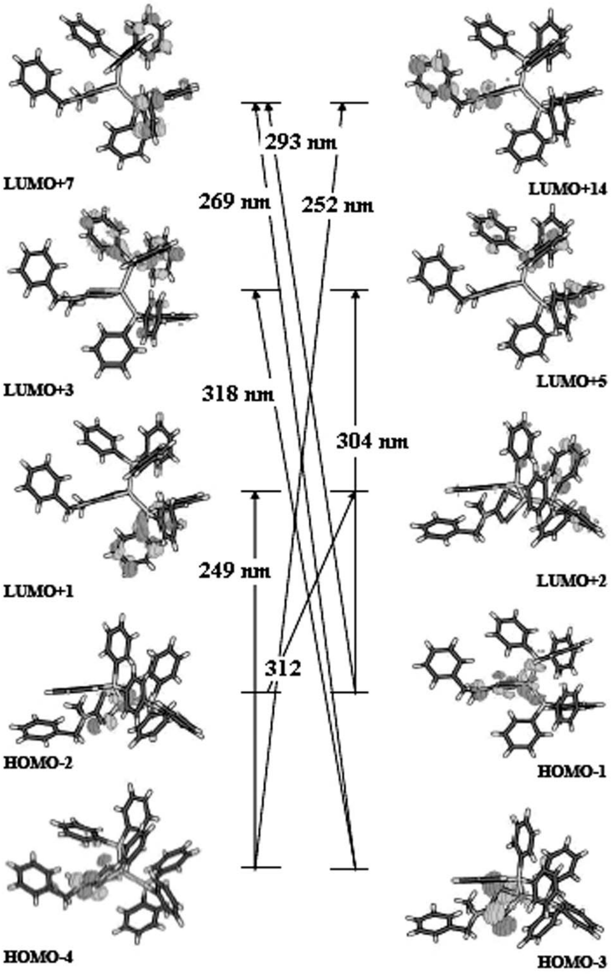

Figure 5. Selected orbital transitions for **2** (orbital contour values are 0.06).

Nonlinear Optical Property

In order to gain some insight into the nonlinear optical property of complex **2** the first static hyperpolarizability (β) was calculated with double numerical differentiation of energies, that is by the finite-field perturbation method. Although 27 components of β can be calculated, only the vector component along the dipole direction is sampled experimentally in the electrical-field-induced second-harmonic generation (EFISH) experiments. The β_{vec} is defined[10] as

$$\beta_{vec} = (\beta_x^2 + \beta_y^2 + \beta_z^2)^{1/2},$$

where β_x, β_y, and β_z are defined as

$$\beta_x = \beta_{xxx} + \beta_{xyy} + \beta_{xzz}$$
$$\beta_y = \beta_{yyy} + \beta_{yxx} + \beta_{yzz}$$
$$\beta_z = \beta_{zzz} + \beta_{zxx} + \beta_{zyy}.$$

Compared with β_{vec} of *p*-nitroaniline (14.44×10^{-30} esu) computed at the same level of theory, **2** (17.88×10^{-30} esu) exhibits stronger second-order polarizability. For **2** the β_x, β_y, and β_z values are -16.23×10^{-30}, 6.69×10^{-30}, and -3.37×10^{-30} esu, respectively. This clearly indicates that the main contribution to β_{vec} arises from the *x*-axis direction for **2**. As indicated in the electronic spectrum of **2** the charge transfer is of ligand-to-ligand type, which is primarily responsible for its good NLO property. For **1** calculations reveal that it is a C_i symmetrical molecule and hence because of the absence of an acentric structure, its β values were not calculated (see Supporting Information).

Pressed Pellet Conductivity

Pressed pellet electrical conductivity studies for both **1** and **2** were performed with a Keithley 236 source measure unit by employing the conventional two-probe technique. Both **1** and **2** are weakly conducting with σ_{rt} values of 2.15×10^{-8} and 5.00×10^{-8} S cm^{-1}, respectively. Their lower conductivity can be attributed to the absence of S···S/M···S intermolecular stacking, which is a prerequisite for the higher conductivity of the complexes (see Supporting Information). A plot of log σ vs. T^{-1} in the 300–343 K temperature range shows their semiconducting behavior. Their conductivity progressively increases with the increase in temperature and ideally decreases vice versa in the given temperature range with bandgaps of 0.94 and 1.24 eV, respectively (Figure 6). The enhancement in σ with temperature may be attributed to the thermal activation of electrons.

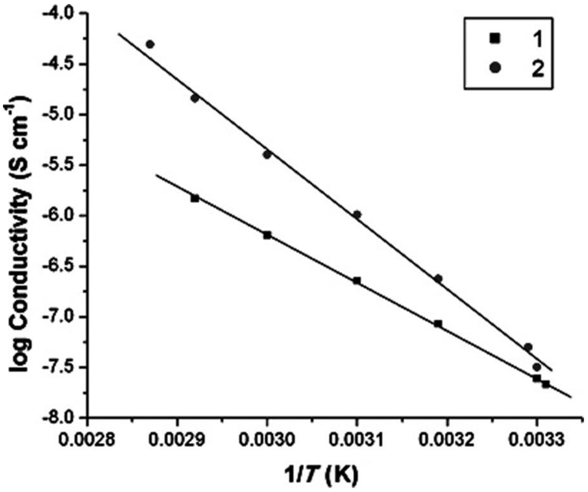

Figure 6. Temperature-dependent pressed pellet conductivity for **1** and **2**.

Conclusions

The TD-DFT calculations for **2** show that the ligand-to-ligand charge transfer transition is primarily responsible for its electronic absorption bands and promising nonlinear optical response. The DFT calculations presented in this paper discern sufficiently good NLO response for **2** due to its asymmetrical structure. These observations may be used for the rational design of new electrooptic materials. Both the compounds are weakly conducting at room temperature because of absence of S···S intermolecular stacking in the solid state and exhibit semiconducting behavior.

Experimental Section

Materials and Reagents: All chemicals were obtained from commercial sources and used as received. The solvents were purified and dried in accordance with the standard literature methods. The precursor $[Cu(PPh_3)_2]NO_3$ was prepared in accordance with the literature procedure[11] while the ligands disodium piperazinedithiocarbamate (Na_2piperzdtc) and sodium *N*-benzyl-*N*-methyldithiocarbamate (NaBzMedtc) were prepared by reacting the appropriate secondary amine with NaOH and CS_2 in appropriate molar ratio in water.

Physical Measurements: Elemental analyses were performed with a Perkin–Elmer 240 C, H, N analyzer. Infrared spectra were recorded as KBr pellets with a Varian 3100 FTIR. ^{1}H, ^{13}C, and ^{31}P NMR spectra were recorded on JEOL AL300 FTNMR spectrophotometers. Chemical shifts were reported in parts per million using TMS as internal standard for ^{1}H and ^{13}C NMR and phosphoric acid for ^{31}P NMR spectra.

Synthesis of $[\{Cu(PPh_3)_2\}_2(\text{piperzdtc})]$ (1): To a stirring dichloromethane solution (50 mL) of $Cu(PPh_3)_2NO_3$ (1.299 g, 2 mmol) was added dropwise methanol solution (40 mL) of the ligand disodium piperazinebis(dithiocarbamate) (0.282 g, 1 mmol) at 0 °C. The solution was additionally stirred for another 30 min to obtain a white residue to which dichloromethane (20 mL) was added. This was filtered and the filtrate was kept for five days to obtain the colorless needle-like crystals, which were filtered and dried (1.10 g, yield 78 %; m.p. 286 °C). $C_{78}H_{68}Cu_2N_2P_4S_4$ (1412.64): calcd. C 66.32, H 4.85, N 1.98; found C 66.28, H 4.02, N 1.23. ^{1}H NMR ($CDCl_3$): δ = 3.87, 3.99. (s, 8 H, ax/eq-NC_4H_8N), 7.22 (m, 60 H, C_6H_5) ppm. ^{13}C NMR ($CDCl_3$): δ = 51.2 (CH_2), 128.4, 128.5, 129.2, 133.6, 133.8, 135.2 (-C_6H_5), 208.2 (-CS_2) ppm. ^{31}P NMR ($CDCl_3$): δ = –1.76 ppm. IR (KBr): $\tilde{\nu}$ = 1091 (ν_{C-S}), 1384 (ν_{C-N}) cm^{-1}.

Synthesis of $[\{Cu(PPh_3)_2\}(\text{BzMedtc})]$ (2): To a stirring dichloromethane solution (30 mL) of $Cu(PPh_3)_2NO_3$ (0.649 g, 1 mmol) was added dropwise a methanol solution (20 mL) of the ligand sodium *N*-benzyl-*N*-methyl dithiocarbamate (0.219 g, 1 mmol) at 0 °C. The solution was additionally stirred for another 30 min and filtered. The filtrate was kept for eight days to obtain the colorless needle-like crystals. This was filtered and dried (0.635 g, yield 81 %; m.p. 171 °C). $C_{45}H_{40}CuNP_2S_2$ (784.43): calcd. C 68.90, H 5.14, N 1.79; found C 69.08, H 5.20, N 1.84. ^{1}H NMR ($CDCl_3$): δ = 3.29 (s, 3 H, CH_3), 5.30 (s, 2 H, CH_2) 7.22 (m, 35 H, C_6H_5) ppm. ^{13}C NMR ($CDCl_3$): δ = 39.7 (CH_3), 57.7 (CH_2), 127.2, 127.7, 128.2, 128.3, 128.5, 129.2 (-PC_6H_5), 133.7, 133.9, 134.5, 134.8, 136.8 (C_6H_5) 209.9 (-CS_2) ppm. ^{31}P NMR ($CDCl_3$): δ = 0.189 ppm. IR (KBr): $\tilde{\nu}$ = 1091 (ν_{C-S}), 1382 (ν_{C-N}) cm^{-1}.

Structure Determination: Intensity data for the colorless crystals **1** and **2** were collected at 105(2) K on a Sapphire2-CCD, OXFORD diffractometer system equipped with graphite-monochromated Mo-K_α radiation (λ = 0.71073 Å). The final unit cell determination, scaling of the data, and corrections for Lorentz and polarization effects were performed with CrysAlis RED.[12] The structures were solved by direct methods (SHELXS-97)[13] and refined by a full-matrix least-squares procedure based on F^2.[14] All non-hydrogen atoms were refined anisotropically; hydrogen atoms were located at calculated positions and refined using a riding model with isotropic thermal parameters fixed at 1.2 times the U_{eq} value of the appropriate carrier atom. Figures for **1** and **2** were prepared using ORTEP.[15] Crystal data for **1**: $C_{78}H_{68}Cu_2N_2P_4S_4$, formula mass 1412.54, triclinic space group $P\bar{1}$, a = 10.2936(4), b = 12.4738(6), c = 14.3842(6) Å, α = 98.306(4), β = 110.233(4), γ = 97.086(4)°, V = 1684.65(13) Å^3, Z = 1, $d_{\mathrm{calcd.}}$ = 1.392 mg m^{-3}, linear absorption coefficient 0.897 $\mathrm{mm^{-1}}$, $F(000)$ = 732, crystal size 0.60 × 0.26 × 0.09 mm, reflections collected 6851, independent reflections 5623 [R_{int} = 0.0209], final indices [$I > 2\sigma(I)$] R_1 = 0.0280 wR_2 = 0.0653, R indices (all data) R_1 = 0.0382, wR_2 = 0.0668, GOF 0.920, largest difference peak and hole 0.404 and –0.281 e Å^{-3}. Crystal data for **2**: $C_{46}H_{40}Cl_2CuNP_2S_2$, formula mass 867.29, triclinic space group $P\bar{1}$, a = 12.2322(7), b = 13.0085(7), c = 15.5313(9) Å, α = 108.702(5), β = 92.990(4), γ = 114.423(5)°, V = 2081.9(2) Å^3, Z = 2, $d_{\mathrm{calcd.}}$ = 1.383 $\mathrm{mg\,m^{-3}}$, linear absorption coefficient 0.864 $\mathrm{mm^{-1}}$, $F(000)$ = 896, crystal size 0.37 × 0.21 × 0.05 mm, reflections collected 9190, independent reflections 7056 [R(int) = 0.0647], final indices [$I > 2\sigma(I)$] R_1 = 0.0453 wR_2 = 0.0614, R indices (all data) R_1 = 0.1288, wR_2 = 0.0711, GOF 0.586, largest difference peak and hole 0.493 and –0.490 e Å^{-3}.

Computational Details: Geometrical characterization of **2** was performed at the level of density functional theory using the B3LYP functional.[16] For the atoms N, S, P, and Cu 6-311G++(d, p) was employed, whereas for C and H 6-31G** basis sets were used. The energies and intensities of the 65 lowest-energy spin-allowed electronic excitations for **2** were calculated using TD-DFT at the same level of theory. The first static hyperpolarizability (β) for **2** was calculated using the finite-field perturbation method. For **1** the calculations were performed by employing the single-crystal X-ray geometry using the Hartree–Fock method. All calculations were performed using the Gaussian 03 program.[17] Molecular orbital diagrams were constructed using the MOLDEN program.[18]

CCDC-712184 (for **1**) and -712185 (for **2**) contains supplementary crystallographic data. These data can be obtained free of charge from The Cambridge Crystallographic Data Centre via www.ccdc.cam.ac.uk/data_request/cif.

Supporting Information (see footnote on the first page of this article): Output files of the theoretical calculations and weak interactions.

Acknowledgments

This work was supported by the Council of Scientific and Industrial Research, New Delhi in the form of Senior Research Fellowship (A. K.) and project no. 01(2032)/06/EMR-II (N. S.). The authors are grateful to Special Assistance Programme (SAP), Department of Chemistry, Faculty of Science, Banaras Hindu University for providing the computational facility.

---

[1] a) D. Cocouvanis, *Prog. Inorg. Chem.* **1979**, *26*, 301–469; b) G. Hogarth, *Prog. Inorg. Chem.* **2005**, *53*, 71–561; c) A. M. Bond, R. L. Martin, *Coord. Chem. Rev.* **1984**, *54*, 23–98; d) A. M. Bond, A. R. Hendrickson, R. L. Martin, J. E. Moir, D. R. Page, *Inorg. Chem.* **1983**, *22*, 3440–3446; e) N. Robertson, L. Cronin, *Coord. Chem. Rev.* **2002**, *227*, 93–127; f) P. Cassoux, L. Valade in *Inorganic Materials* (Eds.: D. W. Bruce, M. O'Hare), 2nd ed., Wiley, Chichester, **1996**; g) A. Kobayashi, E. Fujiwara, H. Kobayashi, *Chem. Rev.* **2004**, *104*, 5243–5264; h) M. Bousseau, L. Valade, J.-P. Legros, P. Cassoux, M. Garbaukas, L. V. Interrante, *J. Am. Chem. Soc.* **1986**, *108*, 1908–1916; i) A. T. Coomber, D. Beljonne, R. H. Friend, J. L. Bredas, A. Charlton, N. Robertson, A. E. Underhill, M. Kurmoo, P. Day, *Nature* **1996**, *380*, 144–146; j) W. Paw, S. D. Cummings, M. A. Mansour, W. B. Connick, D. K. Geiger, R. Eisenberg, *Coord. Chem. Rev.* **1998**, *171*, 125–150; k) N. Singh, A. Prasad, R. K. Sinha, *Inorg. Chem. Commun.* **2006**, *9*, 1058–1062; l) L. Giovagnini, S. Sitran, M. Montopoli, L. Caprrotta, M. Corsini, C. Rosani, P. Zanello, Q. P. Dou, D. Fregona, *Inorg. Chem.* **2008**, *47*, 6336–6343.

[2] a) C. S. Lai, E. R. T. Tiekink, *CrystEngComm* **2003**, *5*, 253–261; b) W. W. H. Wong, D. Curiel, S.-W. Lai, M. G. B. Drew, P. D. Beer, *Dalton Trans.* **2005**, 774–781; c) S.-W. Lai, M. G. B. Drew, P. D. Beer, *J. Organomet. Chem.* **2001**, *637*, 89–93; d) P. D. Beer, N. Bery, M. G. B. Drew, O. D. Fox, M. E. Padilla-Tosta, S. Patell, *Chem. Commun.* **2001**, 199–200; e) W. W. H. Wong, J. Cookson, E. A. L. Evans, E. J. L. McInnes, P. D. Beer, *Chem. Commun.* **2005**, 2214–2216.

[3] N. Singh, A. Kumar, K. C. Molloy, M. F. Mahon, *Dalton Trans.* **2008**, 4999–5007.

[4] S. J. Lippard, *Pure Appl. Chem.* **1987**, *59*, 731–742.

[5] a) D. Cardell, G. Hogarth, S. Faulkner, *Inorg. Chim. Acta* **2006**, *359*, 1321–1324; b) K. Oyaizu, K. Yamamoto, Y. Ishii, E. Tsuchida, *Chem. Eur. J.* **1999**, *5*, 3193–3207; c) M. C. Gimeno, P. G. Jones, A. Laguna, S. Sarroca, M. J. Calherda, J. Veiros, *Chem. Eur. J.* **1998**, *4*, 2308–2314; d) R. Chant, A. R. Hendrickson, R. L. Martin, N. M. Rohde, *Aust. J. Chem.* **1973**, *26*, 2533–2536.

[6] D. F. Lewis, S. J. Lippard, J. A. Zubieta, *Inorg. Chem.* **1972**, *11*, 823–828.

[7] a) F. Shahee, A. Badshah, M. Gieten, M. Dusek, K. FejFarova, D. deVos, B. Mirza, *J. Organomet. Chem.* **2007**, *692*, 3019–3026; b) H. Brunner, T. Burgemeister, J. Washter, *Chem. Ber.* **1975**, *108*, 3349–3354; c) D. Venkappayya, D. H. Brown, *Ind. J. Chem.* **1974**, *12*, 838–839; d) D. H. Brown, D. Venkappayya, *J. Inorg. Nucl. Chem.* **1973**, *35*, 2108–2109; e) L. H. Pignolet, D. T. Duffy, Q. Lawrence Jr., *J. Am. Chem. Soc.* **1973**, *95*, 295–297.

[8] a) J. D. E. T. Wilton-Ely, D. Solanki, E. R. Knight, K. B. Holt, A. L. Thompson, G. Hogarth, *Inorg. Chem.* **2008**, *47*, 9642–9654; b) J. D. E. T. Wilton-Ely, D. Solanki, G. Hogarth, *Eur. J. Inorg. Chem.* **2005**, 4027–4030; c) G. Marcotrigiano, G. C. Pellacani, C. Preti, G. Tosi, *Bull. Chem. Soc. Jpn.* **1975**, *48*, 1018–1020; d) A. Hulanicki, L. Shishkova, *Chem. Anal. (Warsaw)* **1965**, *10*, 837–845.

[9] S. Diez-Gonzilez, S. P. Nolan, *Aldrichimica Acta* **2008**, *41*, 43–51.

[10] S. P. Karna, P. N. Prasad, M. Dupuis, *J. Chem. Phys.* **1991**, *94*, 1171–1181.

[11] G. J. Kubas, *Inorg. Synth.* **1970**, *19*, 90–92.

[12] Oxford Diffraction, *CrysAlis CCD*, *RED*, version 1.711.13, copyright 1995–2003, Oxford Diffraction Poland Sp.

[13] G. M. Sheldrick, *SHELXS97*, Program for Crystal Structure Solution, University of Göttingen, Göttingen, **1997**.

[14] G. M. Sheldrick, *SHELXL97*, Program for Crystal Structure Refinement, University of Göttingen, Göttingen, **1997**.

[15] M. N. Burnett, C. K. Johnson, *ORTEP-III*, Oak Ridge Thermal Ellipsoid Plot Program for Crystal Structure Illustrations, Report ORNL-6895, Oak Ridge National Laboratory, Oak Ridge, TN, USA, **1996**.

[16] a) A. D. Becke, *J. Chem. Phys.* **1993**, *98*, 5648–5652; b) C. Lee, Y. Wang, R. G. Parr, *Phys. Rev. B: Condens. Matter Mater. Phys.* **1988**, *37*, 785–789.

[17] M. J. Frisch, G. W. Trucks, H. B. Schlegel, G. E. Scuseria, M. A. Robb, J. R. Cheeseman, J. A. Montgomery, T. Vreven Jr., K. N. Kudin, J. C. Burant, J. M. Millam, S. S. Iyengar, J. Tomasi, V. Barone, B. Mennucci, M. Cossi, G. Scalmani, N. Rega, G. A. Petersson, H. Nakatsuji, M. Hada, M. Ehara, K. Toyota, R. Fukuda, J. Hasegawa, M. Ishida, T. Nakajima, Y. Honda, O. Kitao, H. Nakai, M. Klene, X. Li, J. E. Knox, H. P. Hratchian, J. B. Cross, V. Bakken, C. Adamo, J. Jaramillo, R. Gomperts, R. E. Stratmann, O. Yazyev, A. J. Austin, R. Cammi, C. Pomelli, J. W. Ochterski, P. Y. Ayala, K. Morokuma, G. A. Voth, P. Salvador, J. J. Dannenberg, V. G. Zakrzewski, S. Dapprich, A. D. Daniels, M. C. Strain, O. Farkas, D. K. Malick, A. D. Rabuck, K. Raghavachari, J. B. Foresman, J. V. Ortiz, Q. Cui, A. G. Baboul, S. Clifford, J. Cioslowski, B. B. Stefanov, G. Liu, A. Liashenko, P. Piskorz, I. Komaromi, R. L.

Martin, D. J. Fox, T. Keith, M. A. Al-Laham, C. Y. Peng, A. Nanayakkara, M. Challacombe, P. M. W. Gill, B. Johnson, W. Chen, W. M. Wong, C. Gonzalez, J. A. Pople, *GAUSSIAN 03* (Revision D.01), Gaussian, Inc., Wallingford, CT, **2004**.

[18] *Molden*, a pre- and post-processing program for molecular and electronic structures: G. Schaftenaar, J. H. Noordik, *J. Comput. Aided Mol. Des.* **2000**, *14*, 123–134.

Received: January 6, 2009